

Battlefield Target Cooperative Deployment Algorithm Based on Improved PSO Multi-Sensor

Chenxuan Wang, Qiuchun Jin

Zhengzhou University of Aeronautics, Zhengzhou, China

Abstract: In modern battlefield environments, precise target monitoring in complex terrains faces challenges of insufficient coverage and low resource utilization efficiency with traditional multi-sensor deployment strategies. This paper proposes an improved Particle Swarm Optimization (PSO)-based multi-sensor cooperative deployment algorithm for battlefield target monitoring, aiming to enhance the overall effectiveness of monitoring systems through intelligent optimization and cooperative sensing. First, a multi-sensor joint detection probability model is constructed, establishing a statistical sensing model incorporating parameters such as sensing radius and adjustment coefficients. Second, a PSO algorithm improved with adaptive inertia weight is introduced, enabling global optimization of sensor positions by dynamically adjusting particle search strategies. Finally, a priority coverage strategy for key areas is designed to ensure 100% monitoring coverage in critical target regions. Simulation experiments demonstrate that compared with random deployment algorithms and standard PSO algorithms, the proposed algorithm increases the effective coverage of monitoring areas from 51.51% to 66.44%, maintains stable 100% coverage in key areas, and significantly enhances target monitoring capabilities and resource utilization efficiency in complex battlefield environments under the same resource conditions, providing an effective solution for multi-sensor cooperative deployment.

Keywords: Multi-Sensor Cooperative Deployment; Battlefield Target Monitoring; Improved Particle Swarm Optimization (PSO)

1. Introduction

In numerous fields such as modern battlefield situational awareness, target monitoring, intelligence collection, and operational

decision-making, multi-sensor cooperative deployment technology serves as the core component for acquiring battlefield information, achieving precise monitoring, and enabling effective decision-making. The scientificity and rationality of deployment strategies directly determine the overall effectiveness of monitoring systems. Traditional multi-sensor deployment methods have been widely applied in battlefield monitoring, including random deployment strategies [1], uniform distribution deployment [2], geometry-based optimization deployment [3], and heuristic algorithm-based deployment [4]. However, when facing complex battlefield environments (such as complex and changeable terrain, irregular target distribution, and priority coverage requirements for key areas), traditional single-model deployment methods often result in insufficient monitoring coverage and low resource utilization efficiency due to their inability to adapt to dynamic battlefield changes in real-time [5]. Against this backdrop, cooperative deployment technology based on intelligent optimization algorithms, which adaptively adjusts sensor positions, has become the core solution for addressing the challenges of target monitoring in complex battlefields [6].

In recent years, the application of Particle Swarm Optimization (PSO) algorithms in multi-sensor deployment has conducted in-depth research focusing on algorithm improvement and deployment efficiency enhancement. Reference [7] constructed a multi-sensor deployment framework based on the standard PSO algorithm, significantly improving deployment accuracy in simple environments by adjusting inertia weight and learning factors. Reference [8] combined PSO with genetic algorithms, enhancing adaptability to complex terrains through hybrid optimization strategies. Reference [9] proposed a lightweight PSO structure based on fuzzy logic, reducing resource consumption while maintaining deployment effectiveness by decreasing

computational complexity. Reference [10] integrated neural network theory, improving deployment accuracy by adaptively adjusting algorithm parameters. Reference [11] designed a dynamic PSO algorithm that dynamically adjusts search strategies based on real-time environmental changes, increasing monitoring coverage by 15% while reducing computational load by 25%. Reference [12] combined PSO with multi-objective optimization theory, constructing a multi-sensor deployment model that balances coverage and resource consumption. These studies indicate that while PSO technology enhances adaptability to complex environments, it still faces challenges in balancing convergence speed and global search capability.

Traditional single-sensor monitoring technology is limited by its single sensing range and environmental noise (such as electromagnetic interference and changing meteorological conditions), often resulting in unsatisfactory monitoring performance that fails to meet the high-precision monitoring requirements of modern battlefields. Although multi-sensor cooperative technology can improve monitoring coverage by optimizing sensor spatial distribution (such as master-slave platform cooperation and priority coverage of key areas) [13], information redundancy and uneven resource allocation among sensors (such as resource waste caused by overlapping sensor positions) still require optimization. The particle swarm optimization algorithm in intelligent optimization theory provides a new approach to address this issue—by simulating swarm intelligence behavior, it can dynamically optimize sensor position layout, avoiding the neglect of global optimality by traditional geometric optimization methods.

This paper proposes an improved PSO-based multi-sensor cooperative deployment algorithm for battlefield target monitoring, addressing the complexity of battlefield environments and the requirements for multi-sensor cooperative deployment. By constructing a multi-sensor joint detection probability model, precise evaluation of monitoring coverage is achieved. Combined with a PSO algorithm improved with adaptive inertia weight, dynamic optimization of sensor position layout is realized. Utilizing a priority coverage strategy for key areas enhances monitoring capabilities for critical targets, providing theoretical support and

technical solutions for multi-sensor cooperative deployment in complex battlefield environments.

2. Node Sensing Model

Although traditional probabilistic sensing models have certain practical applications, considering the performance fluctuations of multi-sensors under different environments and operating conditions, improvements are urgently needed, leading to the emergence of statistical models. First, it is essential to precisely define the sensing radius of multi-sensors, which delineates the approximate range of their effective detection. Simultaneously, clarifying the coordinates of target points enables knowledge of the monitoring object's location, while determining node coordinates lays a solid foundation for constructing data association and transmission systems. These three elements complement each other. Based on these key parameters, researchers have derived the expression for multi-sensor detection probability in statistical models through extensive experiments, data collection, and complex mathematical derivations.

$$C = \begin{cases} 0, & d \geq r_s + r_\delta \\ e^{-\lambda\alpha^\beta}, & r_s - r_\delta < d < r_s + r_\delta \\ 1, & d \leq r_s - r_\delta \end{cases} \quad (1)$$

r_δ is the adjustment coefficient, representing the sensing uncertainty of multi-sensor nodes; λ , β are measurement performance parameters, which are adjustable and have value ranges; Define α , where the detection probability changes in a negative exponential relationship with distance.

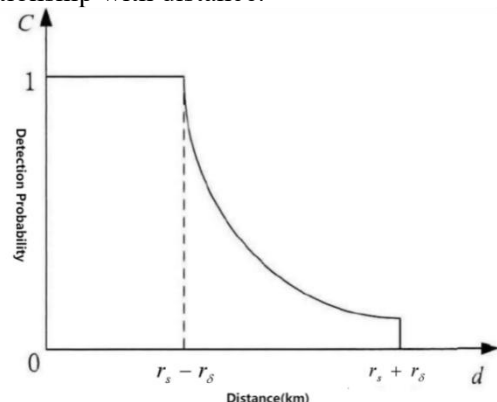


Figure 1. Schematic Diagram of Detection Probability Variation with Distance in Statistical Model

2.1 Analysis of Optimization Indicators

In complex detection scenarios, multi-platform cooperative detection plays a crucial role, while information uncertainty has also become an unignorable challenge. Based on precise directed models, in-depth exploration of multi-sensor deployment algorithms has become the key to breaking the impasse. This algorithm research focuses on optimization indicators. The sensing radius is set to 50 km, the adjustment coefficient is 20 km, and the position coordinates of a certain node are at (80 km, 50 km). The monitoring area is defined as 100 km \times 100 km. Meanwhile, parameters $\lambda = 0.1$ and $\beta = 0.7$ are taken, and the platform carrying multiple sensors moves towards the negative semi-axis of the X-axis. The simulation results of the multi-sensor node statistical model are shown in Figure 2.

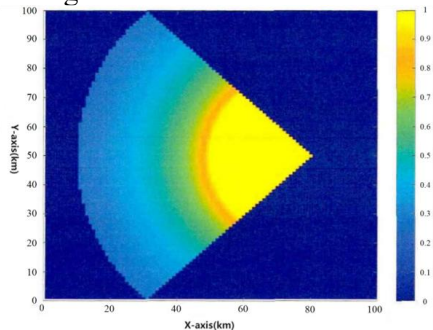


Figure 2. Directed Multi-Sensor Node Statistical Model

As shown in Figure 2, the detection probability is closely related to the distance between the target point and the node. At the node position, due to the most concentrated detection capability of multi-sensors, the probability of target detection reaches the maximum value of 1. Within the sector-shaped area, influenced by the performance radiation of multi-sensors, although the detection probability is not as high as at the node, it still maintains a value greater than 0, ensuring no potential targets are missed. The closer the target point is to the node, the greater the detection probability obtained; conversely, the farther away, the smaller the probability, showing an obvious gradient change.

More importantly, to accurately measure detection effectiveness, C_{th} threshold probability C_{th} is specifically defined. When the target point detection probability C_T is greater than this value, it can be determined as an effectively covered point:

$$C_T \geq C_{th} \quad (2)$$

In the field of multi-sensor detection, when a region meets the conditions set by a specific formula, it is recognized as an effectively covered region. The region's effective coverage

rate R_c based on this definition reflects the proportion of effectively covered regions within the monitoring range. The formula is as follows:

$$R_c = \frac{\text{area}\left(\left(\bigcup_{i \in \eta} A_i\right) \cap M\right)}{\text{area}(M)} \quad (3)$$

$\bigcup_{i \in \eta}$ represents the union of multi-sensor coverage areas; M represents the entire monitoring area; $\left(\bigcup_{i \in \eta} A_i\right) \cap M$ represents the intersection of the union of multi-sensor coverage areas and the monitoring area; $\text{area}\left(\left(\bigcup_{i \in \eta} A_i\right) \cap M\right)$ is the area of the effectively covered region; $\text{area}(M)$ is the area of the entire monitoring region.

The target monitoring area is defined as 100 km \times 100 km, with the x-coordinate ranging from [20 km, 50 km] and the y-coordinate ranging from [30 km, 70 km]. The key area, where critical targets are highly likely to be hidden, is the priority focus range for monitoring resources. In the single-sensor detection scenario, the corresponding model is shown in Figure 3.

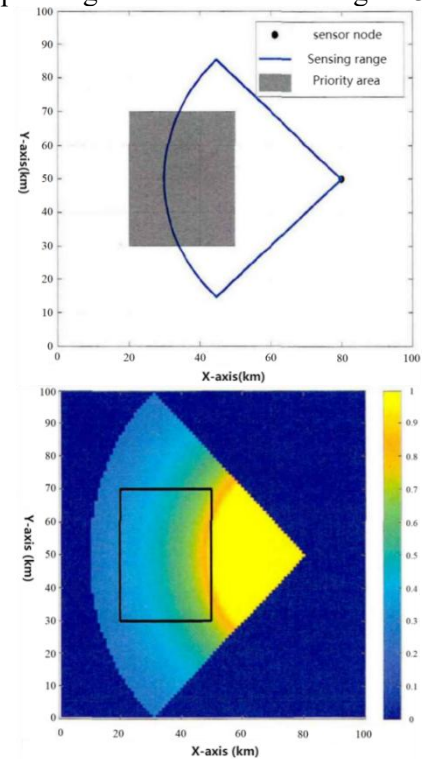


Figure 3. Key Area (Left) and Single Sensor (Right) Node Detection Statistical Model

2.2 Construction of Multi-sensor Cooperative Deployment Algorithm with Improved PSO

The Ant Colony Optimization (ACO) algorithm is based on simulating the cooperative behavior among ant colonies. During foraging, ants leave pheromones to guide their companions toward food sources, and the algorithm uses this mechanism to find optimal solutions. However, its positive feedback process results in prolonged solution time, making it difficult to quickly provide effective solutions in scenarios with high real-time requirements. In comparison, the Particle Swarm Optimization (PSO) algorithm is based on the swarm intelligence behavior of bird flocks during predation. Its principles are easy to understand, it involves fewer parameters, has fast convergence speed, and can efficiently approach optimal solutions. In view of this, this paper selects the PSO algorithm, aiming to optimize multi-sensor deployment and enhance the overall effectiveness and response speed of monitoring systems.

2.2.1 Principle of PSO Algorithm

Particles correspond to potential solutions of the problem to be solved and have matching fitness values. During algorithm execution, particles explore optimal solutions by continuously updating their positions through iterations. The particle swarm consists of n massless particles, possessing two key attributes: velocity and position. These particles can freely move and navigate in a D -dimensional space, leveraging swarm intelligence to collaboratively and efficiently discover the optimal solution to the problem. The iterative state of particles is:

$$x_{i,j}(t+1) = x_{i,j}(t) + v_{i,j}(t+1) \quad (4)$$

$pbest_{i,j}(t)$ represents the best position found so far for the i -th particle, while $gbest_j(t)$ is the best position found so far among all particles.

In particle swarm optimization, the memory term causes the particle's velocity to be significantly influenced by the velocity of parent particles, enabling particles to gradually approach the optimal solution in a directed manner. The inertia weight factor ω can effectively enhance local search capability and precisely locate the optimal solution; conversely, a larger ω improves global search capability. Learning factors c_1 and c_2 ensure that particles

balance exploration of new regions and in-depth exploitation. Adding random numbers r_1 and r_2 between 0 and 1 makes the exploration path more varied, comprehensively enhancing the algorithm's optimization performance. A new guidance mechanism is introduced in the optimization process of the particle swarm algorithm, using the particle's neighborhood best position as the social cognition guide. In traditional algorithms, particles often adjust themselves based on the global best position, while this approach focuses on the local neighborhood where the particle is located, extracting optimal position information within it. During the velocity update phase, particles no longer solely pursue the global optimum but instead refer more to nearby particles, a strategy known as the local best particle swarm optimization algorithm. In complex and dynamic search scenarios, this allows particles to find the optimal path that suits them faster and more accurately. The velocity update is defined as:

$$v_{i,j}(t+1) = \omega v_{i,j}(t) + c_1 r_1 (pbest_{i,j} - x_{i,j}) + c_2 r_2 (gbest_j - x_{i,j})$$

where $gbest_j$ is the best position within the neighborhood of the i -th particle.

2.2.2 Algorithm Improvement

When applying the Particle Swarm Optimization (PSO) algorithm to solve problems, its parameter values must closely align with the characteristics of the actual problem. Minor adjustments to different parameters can significantly impact the algorithm's performance and efficiency. This chapter optimizes the standard algorithm by adopting an adaptive inertia weight coefficient to update particle states, breaking the limitations of traditional fixed parameters. This allows particles to flexibly adjust according to real-time conditions during the search process, enabling the algorithm to find optimal solutions when facing complex and dynamic multi-sensor deployment challenges. The expression for the adaptive inertia weight coefficient ω is as follows:

$$\omega = \begin{cases} \omega_{\min} - \frac{(\omega_{\max} - \omega_{\min}) \times (f_c - f_{\min})}{(f_{\text{avg}} - f_{\min})}, & f_c \geq f_{\text{avg}} \\ \omega_{\max}, & f_c < f_{\text{avg}} \end{cases} \quad (5)$$

where f_c represents the particle's fitness function value; f_{avg} , f_{\min} represent the

average and minimum fitness, respectively. The inertia weight typically ranges from [0.4, 0.9]. In the later stages of the search, by reducing the inertia weight, particles focus on local region improvement and gradually approach the global optimal solution. In the early stages of the search, increasing the inertia weight provides particles with stronger global search capabilities, enabling them to quickly locate potential high-quality regions. The adaptive adjustment strategy dynamically balances global and local exploration capabilities according to the search phase, allowing the algorithm to converge to the optimal solution at a faster speed. The detailed operation process of the improved algorithm is shown in Figure 4.

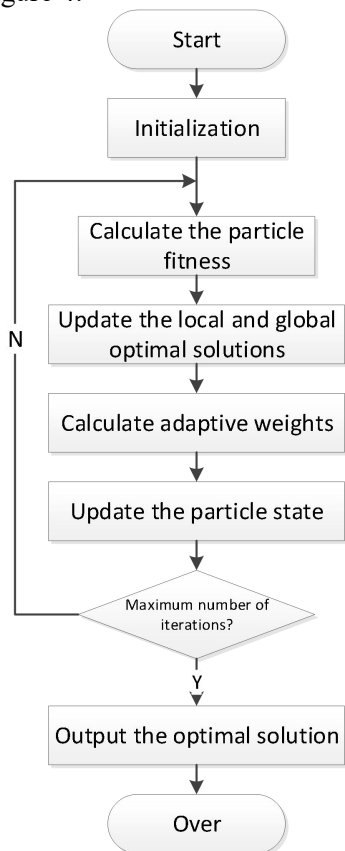


Figure 4. Flowchart of Improved Particle Swarm Optimization Algorithm

In multi-sensor battlefield target deployment tasks, the improved particle swarm optimization algorithm ensures precise detection of key areas. Through optimized search strategies, it enables efficient allocation of multi-sensor resources and significantly improves the effective coverage of key areas. By means of adaptive adjustment of particle states and reasonable optimization of parameters, it derives scientifically reasonable multi-sensor deployment plans.

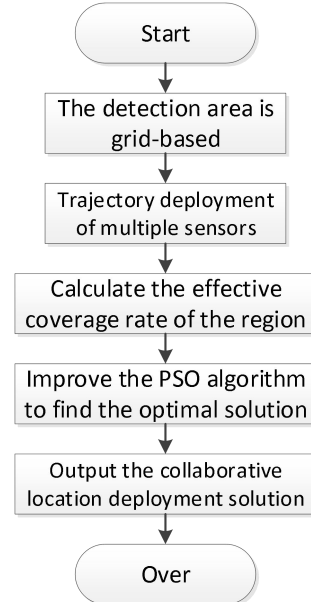


Figure 5. Flowchart of Multi-Sensor Cooperative Deployment Algorithm based on Improved Particle Swarm Optimization

The process of the improved algorithm is as follows:

Step 1: Area Gridding

For precise monitoring, divide the target area into a uniform grid with a precisely set side length of 5 km.

Step 2: Multi-sensor Deployment

Adopt a random strategy to place multi-sensors at grid nodes.

Step 3: Initial Performance Evaluation

Immediately after deployment, calculate the joint detection probability and coverage rate to evaluate the detection effectiveness.

Step 4: Algorithm-driven Optimization

Select the coverage rate as the fitness function and utilize the improved particle swarm optimization algorithm to perform optimization.

Step 5: Solution Output

When the iteration reaches the maximum number of times, the output deployment plan is the optimal solution that meets the monitoring requirements.

3 Simulation Experiments

3.1 Simulation Experiment of Multi-Sensor Random Deployment Target Algorithm

In this detection mission, the platform flies steadily along the negative semi-axis of the X-axis. The target monitoring area is 100 km × 100 km, with the central 20 km × 20 km area having extremely high requirements for detection accuracy and frequency. To achieve

efficient detection, a battlefield target cooperative detection system is constructed, consisting of one master platform leading and two slave platforms assisting. The master platform is responsible for overall coordination, integrating data from all parties, and arranging tasks, while the slave platforms are specifically responsible for partial area detection and auxiliary verification. The system is equipped with $M = 3$ multi-sensors, namely S_1 , S_2 , and S_3 .

Table 1. Simulation Parameter Table for Multi-Sensor Random Deployment Algorithm

Parameter	Details
Sensing Radius	Master platform: 70 km, Slave platforms: 50 km
Adjustment Coefficient	20km
Adjustable Parameter λ	0.1
Adjustable Parameter β	0.7

In the simulation experiment, the multi-sensor positions, sensing ranges, and detection probabilities are shown in Figure 6 below.

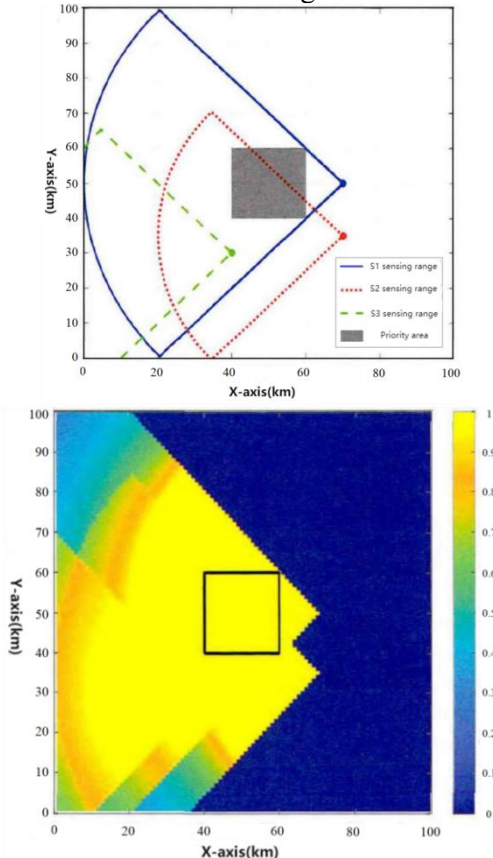


Figure 6. Schematic Diagram of Sensor Positions and Sensing Ranges (Left), Sensor Detection Probabilities (Right)

In the multi-sensor random deployment experiment shown in Figure 3.29, the detection probability exhibits severe polarization within

the area. Some regions, due to multi-sensor cooperation, are constantly under high-intensity monitoring; while other regions, being far from multi-sensors, have detection probabilities close to zero. The experiment sets the threshold probability at 0.5. When the value exceeds 0.5, it indicates that targets can be precisely detected with high probability. High detection probability areas and above-threshold areas have equivalent practical effects, both possessing reliable detection capabilities. From the overall effectiveness perspective, the overall coverage rate of this experiment is 51.51%, and the key area achieves 100% coverage, ensuring no critical targets are missed. Fifty Monte Carlo experiments are conducted for the multi-sensor random deployment algorithm, and the effective coverage rates of the monitoring area and key area are shown in Figure 7.

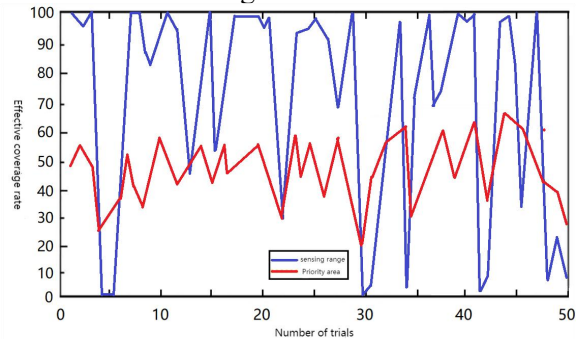


Figure 7. Effective Coverage Rate of Random Deployment Experiment Area

In the multi-sensor random deployment experiment shown in Figure 7, the effective coverage rate of the area exhibits extreme instability across multiple repeated experiments. The overall coverage rate fluctuates significantly between 25% and 65%, and in most cases only maintains around 50%. The coverage rate of key areas also shows large fluctuations. The low coverage rate is attributed to the random deployment method of multi-sensors. Due to the randomness of their positions, severe overlap phenomena occur frequently. Multi-sensors cluster in certain areas, lacking effective cooperation between sensors and failing to form complementary advantages of repeated detection. There is an urgent need to introduce a cooperative mechanism to reduce mutual overlap and improve joint detection probability.

3.2 Simulation Experiment of Multi-Sensor Cooperative Deployment Algorithm Based on Standard Particle Swarm Optimization

Assume the platform flies along the negative semi-axis of the X-axis within a square area of $100 \text{ km} \times 100 \text{ km}$. In the center of this area, a $20 \text{ km} \times 20 \text{ km}$ region is designated as the key area. The entire system includes 1 master platform and 2 slave platforms, equipped with multi-sensors. In terms of data processing, the threshold probability is set to 0.5, with 70 iterations performed. The fitness function, as the key to evaluating system performance, includes two indicators, each assigned corresponding weights. In this way, during flight, each

platform and multi-sensor cooperate with each other, using the threshold probability as the judgment basis, undergoing 70 iterations, and continuously optimizing the monitoring and data analysis tasks for the $100 \text{ km} \times 100 \text{ km}$ area, especially the central $20 \text{ km} \times 20 \text{ km}$ key area, based on the two indicators of the fitness function with set weights. The fitness function for standard particle swarm optimization is constructed as:

$$f = k_1 R_{c_key} + k_2 R_{c_all} \quad (3.10)$$

The simulation parameters are shown in Table 2.

Table 2. Simulation Parameters

Category	Details		
Multi-sensor Parameters	Sensing radius: Master platform 70 km, Slave platforms 50 km; Adjustment coefficient: 20 km; Adjustable parameter λ : 0.1; Adjustable parameter β : 0.7		
Standard Particle Optimization Algorithm Parameters	Number of particles: 30; Inertia weight: 0.9; Learning factor: 2; Indicator weight k_1 : 0.5; Indicator weight k_2 : 0.5		

The multi-sensor positions, sensing ranges, and multi-sensor detection probabilities are shown in Figure 8 below.

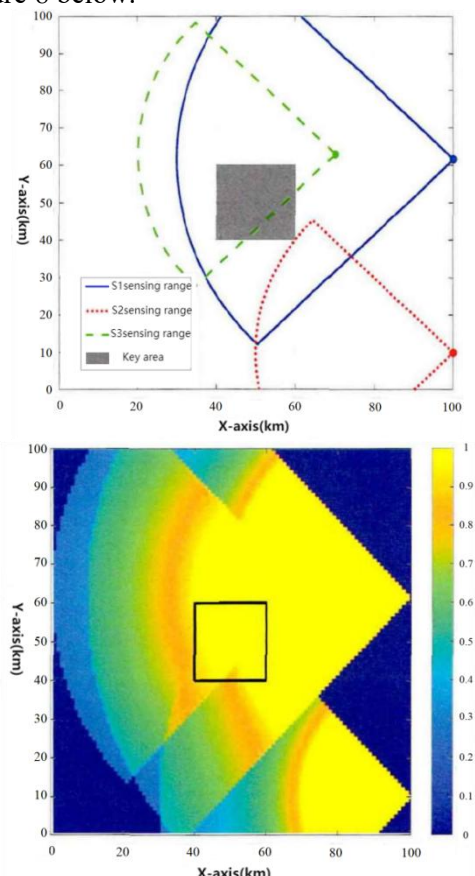


Figure 8. Cooperative Deployment Experiment of Multi-Sensor Positions and Sensing Ranges (Left), Multi-Sensor Detection Probabilities (Right)

Figure 8 clearly illustrates the scenario where

sensor positions are deployed in a more distributed manner. This distributed deployment brings significant advantages, enabling the utilization rate of multi-sensors to be enhanced, thereby effectively improving the overall coverage rate. Figure 3.32 further demonstrates the variation diagram of coverage rate in an intuitive manner.

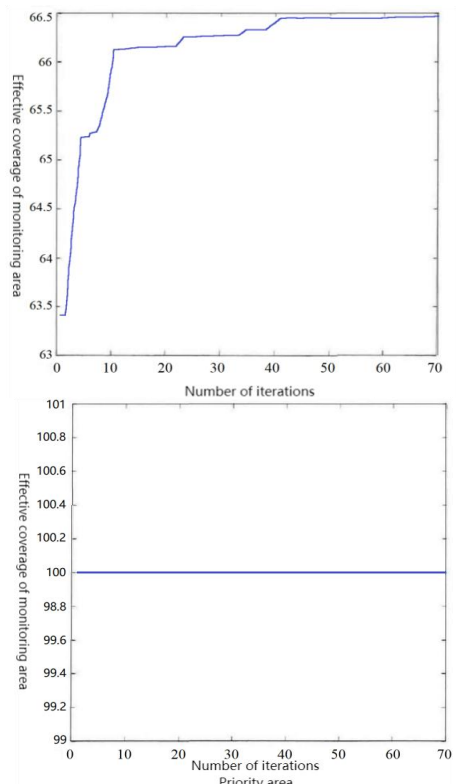


Figure 9 Multi-sensor positions and sensing ranges

As can be seen from Figure 9, as the number of

iterations increases, the effective coverage rate of the monitoring area improves accordingly. At the completion of iterations, the effective coverage rate of the entire monitoring area is calculated to be 66.44%; the effective coverage rate of the key area remains consistently at 100% throughout the iteration process.

A balance optimization experiment is conducted based on the standard algorithm, with the set conditions kept consistent with those in Experiment (2). During the iteration process, a unique calculation method is used to determine the adaptive weight, thereby achieving dynamic updates of particle states. This optimization strategy is visually presented in Figure 9, where 9(a) clearly shows the optimized deployment situation, allowing observation of key information such as particle distribution and position layout. Figure 9(b) focuses on displaying the detection probability, which reflects the likelihood of different areas or targets being accurately detected under the current deployment.

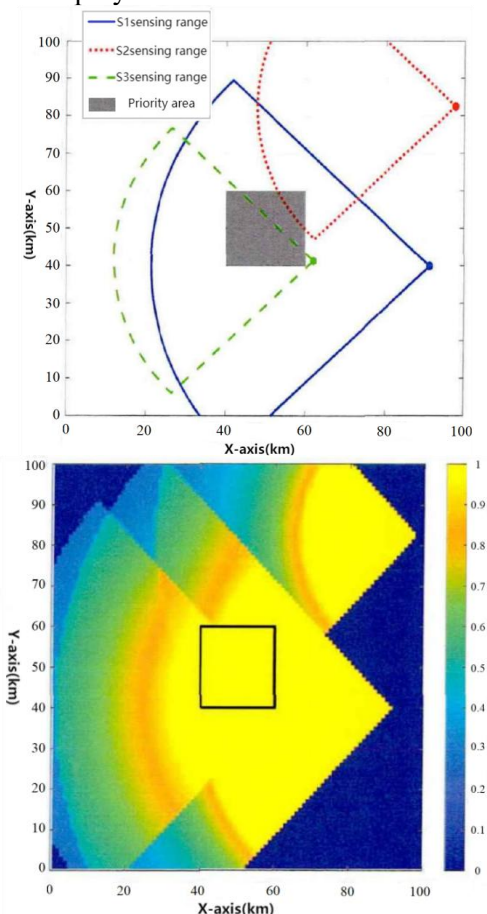


Figure 10. Cooperative Deployment Experiment of Multi-Sensor Positions And Sensing Ranges (Left), Multi-Sensor Detection Probabilities (Right)

According to Figure 10, the two algorithms demonstrate a high degree of similarity in multi-sensor deployment positions, indicating that both algorithms perform excellently in resource utilization. They are both able to fully tap resource potential and effectively expand the joint detection probability. Figure 10, through the coverage rate variation diagram, presents a dynamic perspective showing the impact of the two algorithms on the coverage range under different times or conditions.

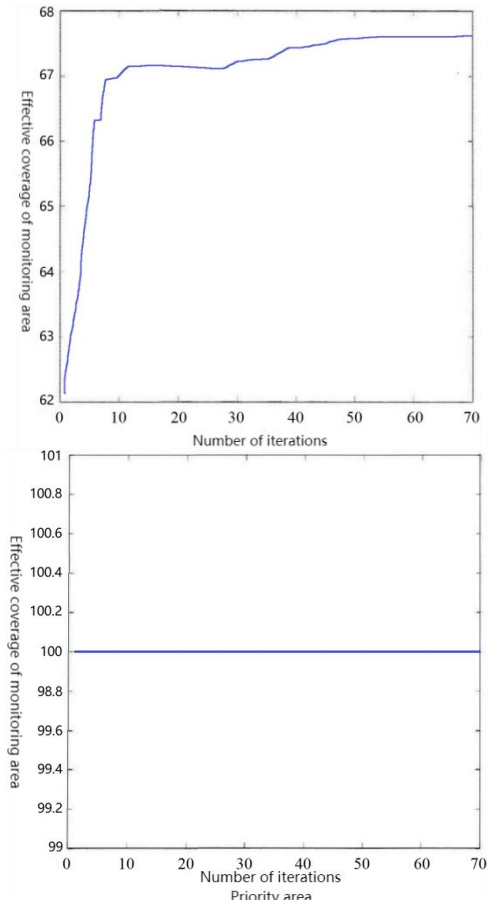


Figure 11. Cooperative Deployment Coverage Rate of Multi-Sensor Positions and Sensing Ranges (Left), Multi-Sensor Detection Probabilities (Right)

Figure 11 clearly shows that as the number of iterations continuously increases, the coverage rate of the monitoring area steadily rises, and the coverage rate of the key area reaches 100%. By combining the analysis of Figures 3.32 and 3.34, it can be found that both algorithms demonstrate significant advantages in coverage rate compared to random deployment. Under the same resource conditions, these two algorithms can effectively reduce detection blind spots and greatly improve the comprehensiveness and accuracy of monitoring. Further comparing the

standard algorithm with the improved algorithm, the standard algorithm adopts a constant inertia weight, while the improved algorithm utilizes an adaptive inertia weight. Figure 3.35 specifically provides a visual comparison of the inertia weights of these two algorithms.

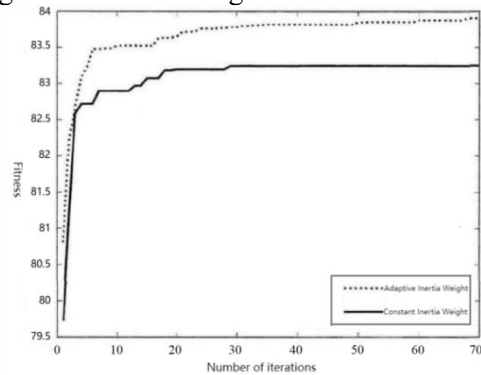


Figure 12. Comparative Schematic Diagram of Fitness Variation During Iteration Process

Figure 12 clearly shows that as the number of iterations continuously increases, the coverage rate of the monitoring area steadily rises, and the coverage rate of the key area reaches 100%. By combining the analysis of Figures 9 and 11, it can be found that both algorithms demonstrate significant advantages in coverage rate compared to random deployment. Under the same resource conditions, these two algorithms can effectively reduce detection blind spots and greatly improve the comprehensiveness and accuracy of monitoring. Further comparing the standard algorithm with the improved algorithm, the standard algorithm adopts a constant inertia weight, while the improved algorithm utilizes an adaptive inertia weight. Figure 12 specifically provides a visual comparison of the inertia weights of these two algorithms.

References

- [1] Singh, S. P., & Sharma, S. C. (2018). A PSO based improved localization algorithm for wireless sensor network. *Wireless Personal Communications*, 98(1), 487-503.
- [2] Wang, Jin, et al. "A PSO based energy efficient coverage control algorithm for wireless sensor networks." *Computers, Materials & Continua* 56.3 (2018).
- [3] Vimalarani, C., R. Subramanian, and S. N. Sivanandam. "An enhanced PSO-based clustering energy optimization algorithm for wireless sensor network." *The Scientific World Journal* 2016.1 (2016): 8658760.
- [4] Zhao, Qiang, et al. "Coverage optimization of wireless sensor networks using combinations of PSO and chaos optimization." *Electronics* 11.6 (2022): 853.
- [5] Lee, Shu-Hung, et al. "PSO-based target localization and tracking in wireless sensor networks." *Electronics* 12.4 (2023): 905.
- [6] Sharmin, Sharmin, Ismail Ahmedy, and Rafidah Md Noor. "An energy-efficient data aggregation clustering algorithm for wireless sensor Networks using hybrid PSO." *Energies* 16.5 (2023): 2487.
- [7] Subramani, Shalini, and M. Selvi. "Multi-objective PSO based feature selection for intrusion detection in IoT based wireless sensor networks." *Optik* 273 (2023): 170419.
- [8] Tripathy, Pujasuman, and P. M. Khilar. "PSO based Amorphous algorithm to reduce localization error in Wireless Sensor Network." *Pervasive and Mobile Computing* 100 (2024): 101890.
- [9] Vimalarani, C., R. Subramanian, and S. N. Sivanandam. "An enhanced PSO-based clustering energy optimization algorithm for wireless sensor network." *The Scientific World Journal* 2016.1 (2016): 8658760.
- [10] Batool, Mouazma, Ahmad Jalal, and Kibum Kim. "Sensors technologies for human activity analysis based on SVM optimized by PSO algorithm." *2019 international conference on applied and engineering mathematics (ICAEM)*. IEEE, 2019.
- [11] Guo, Wenzhong, et al. "A PSO-optimized real-time fault-tolerant task allocation algorithm in wireless sensor networks." *IEEE Transactions on Parallel and Distributed Systems* 26.12 (2014): 3236-3249.
- [12] Lakshmi, Yedida Venkata, et al. "Accurate range-free localization with hybrid DV-hop algorithms based on PSO for UWB wireless sensor networks." *Arabian Journal for Science and Engineering* 49.3 (2024): 4157-4178.
- [13] Bansal, Shikha. "Performance Optimization and Design of a Fire Extinguisher Wireless Sensor Drone System Using Petri Nets Modeling and PSO Algorithm." *IEEE Sensors Journal* (2024).
- [14] Li, Guolin, et al. "A near-infrared trace hydrogen sulfide sensor based on CEEMDAN and PSO-LSSVM." *Microwave and Optical Technology Letters* 65.5 (2023): 1047-1053.